Lysine-specific demethylase 1 (LSD1) suppresses cellular senescence by riboflavin uptake-dependent demethylation activity

Osumi, Taiichi ; Nagano, Taiki ; Iwasaki, Tetsushi ; Nakanishi, Jotaro ; Miyazawa, Kazuyuki ; Kamada, Shinji

(Citation)
Scientific Reports,15(1):6525

(Issue Date)
2025-02-23

(Resource Type)
journal article

(Version)
Version of Record

(URL)
https://hdl.handle.net/20.500.14094/0100493334

scientific reports

Check for updates

OPEN

Lysine-specific demethylase 1 (LSD1) suppresses cellular senescence by riboflavin uptake-dependent demethylation activity

Taiichi Osumi[1], Taiki Nagano[2], Tetsushi Iwasaki[1,2], Jotaro Nakanishi[3], Kazuyuki Miyazawa[3] & Shinji Kamada[1,2]✉

Cellular senescence is defined as a permanent proliferation arrest caused by various stresses, including DNA damage. We have recently identified the riboflavin transporter SLC52A1, whose expression is increased in response to senescence-inducing stimuli. Interestingly, increased expression of SLC52A1 suppresses cellular senescence through the uptake of riboflavin and an increase in intracellular flavin adenine dinucleotide (FAD), an enzyme cofactor synthesized from riboflavin. However, how FAD suppresses cellular senescence has not been fully elucidated. Therefore, in this study, we focused on lysine-specific demethylase 1 (LSD1), which uses FAD as a cofactor. First, we found that LSD1 inhibition promoted DNA damage-induced cellular senescence, whereas ectopic expression of LSD1 suppressed cellular senescence, suggesting that LSD1 suppresses senescence. In addition, the demethylation activity of LSD1 against histone H3 and p53 was increased by senescence-inducing stress in a riboflavin uptake-dependent manner. Furthermore, it was revealed that the LSD1 demethylation activity was required for suppression of pro-senescence genes *Sirtuin-4* and *p21* whose expression is modified by methylation status of histone H3 and possibly p53, respectively. Collectively, these results suggest that the FAD increase by senescence-inducing stress leads to LSD1-mediated demethylation of histone H3 and p53, which results in the suppression of pro-senescence genes to inhibit senescence induction.

Keywords LSD1, Demethylation, Cellular senescence, Riboflavin, Flavin adenine dinucleotide (FAD), DNA damage

Cellular senescence is a state of cell cycle arrest caused by a variety of stresses, including DNA damage, telomere shortening, loss of epigenetic information, and oxidative stress[1–3]. Senescent cells accumulate in the body with age and cause age-related diseases through the secretion of proinflammatory cytokines[4]. Because the exact mechanism of cellular senescence remains unclear, elucidation of the mechanisms that induce cellular senescence is necessary for developing treatments for age-related diseases. Recently, we have demonstrated that the riboflavin transporter SLC52A1 (also known as GPR172B/RFVT1) is upregulated in a p53-dependent manner in response to senescence-inducing stimuli and contributes to the suppression of senescence[5]. Riboflavin is a water-soluble B vitamin that is metabolically converted within cells to flavin mononucleotide (FMN) and then to flavin adenine dinucleotide (FAD)[6]. FAD is a coenzyme that catalyzes biological redox reaction in cells[7]. Interestingly, senescence-inducing stimuli have also been shown to increase intracellular FAD levels in an SLC52A1-dependent manner[8]. Thus, FAD-dependent enzyme(s) are considered to act to suppress senescence, but it is unclear which enzyme(s) are responsible.

On the other hand, lysine-specific demethylase 1 (LSD1; also known as KDM1A/AOF2) is a histone demethylase that specifically removes mono- or dimethyl groups from histone H3 lysine 4 (H3K4) and H3 lysine 9 (H3K9) using FAD as a coenzyme[9]. These epigenetic modifications have been reported to regulate the expression of downstream genes[10] and affect the cell cycle and senescence. For example, LSD1 suppresses the expression of Sirtuin-4, a nicotinamide adenine dinucleotide (NAD)-dependent deacetylase, that triggers

[1]Department of Biology, Graduate School of Science, Kobe University, 1-1 Rokkodai-cho, Nada-ku, Kobe 657-8501, Japan. [2]Biosignal Research Center, Kobe University, 1-1 Rokkodai-cho, Nada-ku, Kobe 657-8501, Japan. [3]MIRAI Technology Institute, Business Core Technology Center, Shiseido Co., LTD, 1-2-11 Takashima, Nishi-ku, Yokohama 220-0011, Japan. ✉email: skamada@kobe-u.ac.jp

senescence[11]. LSD1 also accelerates the expression of E2F1 target genes, such as MYC and AKT3, thereby promoting S-phase entry[12]. In addition, LSD1 has been reported to post-translationally modify non-histone proteins, including demethylation of p53, a critical transcription factor that induces senescence. By demethylating p53 lysine 370 (p53K370), LSD1 suppresses the interaction of p53 with its coactivator 53BP1, thereby inhibiting the transcriptional function of p53[13]. However, the relationship between LSD1 and FAD-mediated suppression of senescence has yet to be elucidated.

In this study, we explored the functional significance of LSD1 in FAD-mediated senescence suppression. As a result, we found that LSD1 is activated depending on riboflavin taken up by SLC52A1, which inhibits cellular senescence through its demethylation activity.

Results

LSD1 inhibition promotes DNA damage-induced senescence

To investigate the possible function of LSD1 in cellular senescence, we evaluated the effect of LSD1 knockdown in osteosarcoma U2OS cells, a human tumor cell line (Fig. 1a–e). As previously reported[5], a sublethal dose of etoposide (2 μM), a potent anti-cancer compound that increases DNA breaks, effectively induced senescence in U2OS cells, as determined by widely used senescence markers, activation of senescence-associated β-galactosidase (SA-β-gal)[14] and loss of proliferative capacity. At the same condition, we further confirmed that the increase of γH2A.X foci, a DNA damage marker (Fig. S1a), and the increase of p53 expression, a transcription factor that is important for senescence induction (Fig. S1b). U2OS cells transfected with siRNA for *LSD1* were treated with etoposide, and the efficacy of *LSD1* knockdown was confirmed by quantitative PCR (qPCR) and immunoblot analysis (Fig. 1a). We observed that LSD1 knockdown promoted SA-β-gal activation (Fig. 1b) and reduced EdU-positive cells (Fig. 1c). In addition, qPCR and immunoblot analysis showed that *LSD1* knockdown increased etoposide-induced upregulation of *p21*, a factor required for senescence induction (Fig. 1d). Furthermore, qPCR analysis showed that etoposide-induced upregulation of *IL-6* and *IL-8*, the so-called senescence-associated secretory phenotype (SASP) factors, was also increased by *LSD1* knockdown (Fig. 1e). These results suggest that LSD1 depletion promotes senescence.

To examine whether the catalytic activity of LSD1 is required for the suppression of cellular senescence, we next used ORY-1001, a highly selective LSD1 inhibitor[15], to investigate the effect of LSD1 inhibition on senescence (Fig. 1f–i). ORY-1001 promoted SA-β-gal activation and tended to reduce proliferation ability in etoposide-treated U2OS cells (Figs. 1f,g, and S2a,b). In addition, qPCR and immunoblot analysis showed that LSD1 inhibition also increased etoposide-induced upregulation of *p21* (Fig. 1h). Furthermore, qPCR analysis revealed that etoposide-induced upregulation of *IL-6* and *IL-8* was also enhanced by LSD1 inhibition (Fig. 1i). These results suggest that catalytic inhibition of LSD1 promotes DNA damage-induced senescence in U2OS cells.

To assess the generality of the finding that depletion of LSD1 promotes cellular senescence in U2OS cells, we performed a similar assay in normal human fibroblast Hs68 cells (Fig. S3). Hs68 cells transfected with siRNA against *LSD1* were treated with etoposide, and the efficacy of *LSD1* knockdown was confirmed by qPCR and immunoblot analysis (Fig. S3a). As is in U2OS cells, 2 μM etoposide effectively induced senescence in Hs68 cells, leading to activation of SA-β-gal and loss of proliferative capacity (Fig. S3b,c). Importantly, we observed that *LSD1* knockdown promoted SA-β-gal activation (Fig. S3b) and reduced EdU-positive cells in etoposide-treated cells (Fig. S3c). In addition to *IL-6* and *IL-8*, we found that the expression levels of matrix metalloproteinases *MMP1* and *MMP3*, which are widely known as SASP factors, were increased by *LSD1* knockdown in etoposide-treated Hs68 cells (Fig. S3d). These results indicate that LSD1 inhibition promotes DNA damage-induced senescence, regardless of cell type and whether the cells are cancerous or normal.

Overexpression of LSD1 suppresses cellular senescence

To further evaluate the role of LSD1 in cellular senescence, an expression vector carrying *LSD1* was introduced into U2OS cells, and the degree of senescence was assessed by senescence markers (Fig. 2). The efficacy of LSD1 overexpression was confirmed by immunoblot analysis (Fig. 2a). Notably, overexpression of LSD1 inhibited etoposide-induced SA-β-gal activation (Fig. 2b). Furthermore, etoposide-induced upregulation of p21 was suppressed by LSD1 overexpression at both the mRNA and protein levels (Fig. 2c). These results suggest that overexpression of LSD1 suppresses DNA damage-induced senescence.

LSD1 is activated in response to senescent stress

As previously reported[8], FAD, a cofactor made from riboflavin, increases in response to senescent stress. We next examined whether LSD1 is activated in response to senescent stress. LSD1 specifically removes methyl groups from mono- or dimethylated histone H3K4 and H3K9[9]. To examine the activation of LSD1, U2OS cells were transfected with siRNA for *LSD1*, and the levels of monomethylated histone H3 lysine 4 (H3K4me1) and H3 lysine9 (H3K9me1), and dimethylated histone H3 lysine 4 (H3K4me2) and H3 lysine9 (H3K9me2) were assessed by immunoblot analysis. Knockdown of *LSD1* led to an increase in methylation levels of H3K4 and H3K9 in etoposide-treated cells but not in untreated cells (Fig. 3a), suggesting that LSD1 is involved in demethylation of H3K4 and H3K9 in etoposide-treated cells. We next set out to examine the relationship between histone methylation levels and Sirtuin-4, a known direct target gene of LSD1. Sirtuins are conserved NAD-dependent protein deacetylase/ADP-ribosyltransferase family, and among the sirtuins, Sirtuin-4 promotes senescence by reducing glutamine repletion and mitochondrial function[11]. As shown in Fig. 3b, the expression of *Sirtuin-4* was enhanced by *LSD1* knockdown in etoposide-treated cells. These results suggest that LSD1 activated in response to senescent stress suppresses senescence through histone demethylation and inhibition of *Sirtuin-4* expression. To confirm this, we tested the effect of pharmacological inhibition of LSD1 on histone demethylation following etoposide treatment. In cells treated with ORY-1001 after etoposide treatment, histone methylation

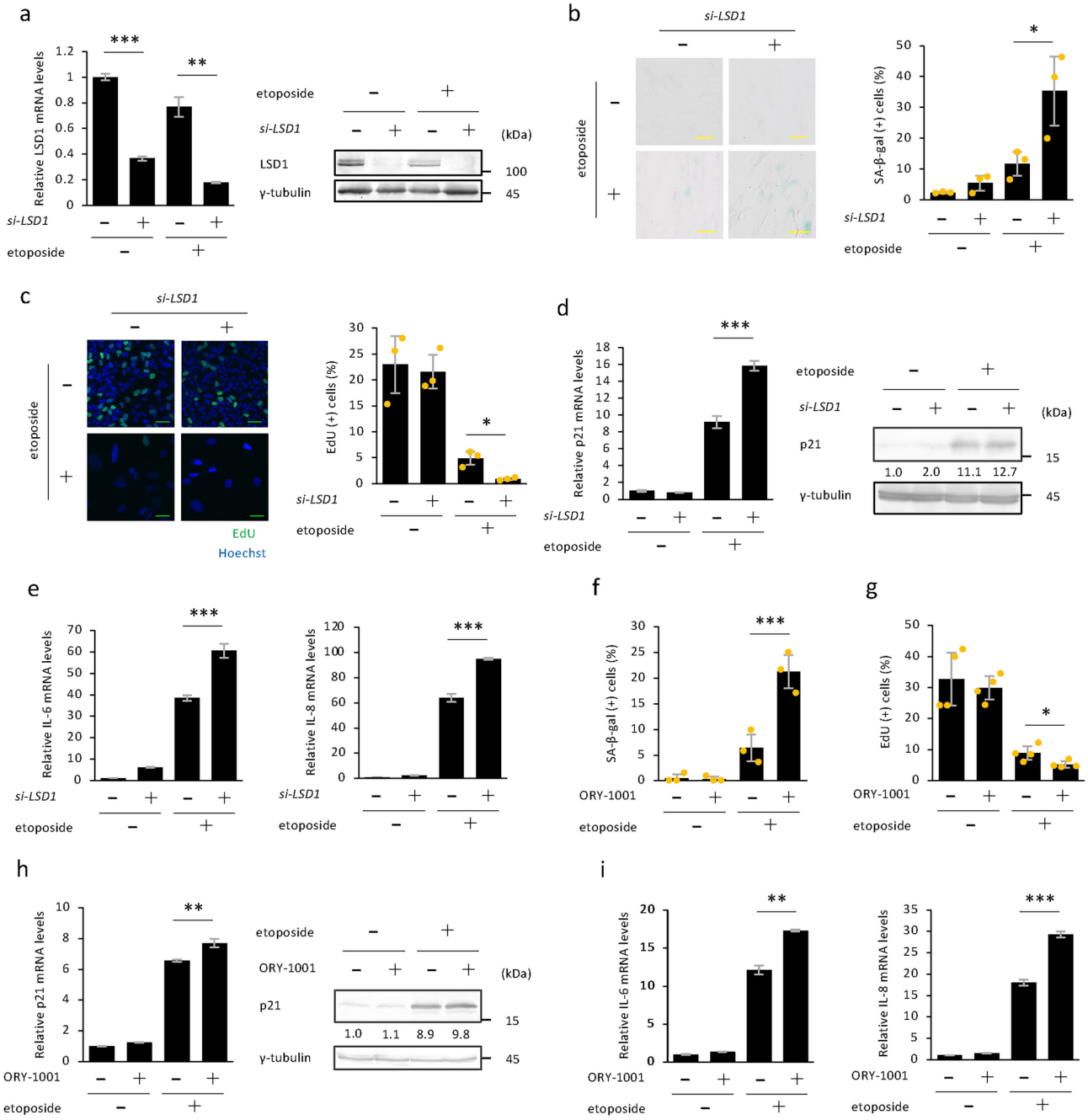

Fig. 1. LSD1 inhibition promotes DNA damage-induced senescence in U2OS cells. (**a**) U2OS cells transfected with siRNA for *LSD1* and treated with 2 μM etoposide for 7 days were subjected to qPCR (left panel) and immunoblot analysis (right panel). (**b**, **c**) *LSD1*-depleted U2OS cells treated with 2 μM etoposide for 7 days were subjected to SA-β-gal (**b**) and EdU (**c**) assays. Representative microscopic images (**b** and **c**, left panels) and the percentage of SA-β-gal positive cells (**b**, right panel) and EdU positive cells (**c**, right panel) are shown. Bars, 50 μm. (**d**) Gene expression of *p21* in *LSD1*-depleted U2OS cells treated with 2 μM etoposide for 6 days was examined by qPCR (left panel) and immunoblot analysis (right panel). (**e**) Gene expression of *IL-6* (left panel) and *IL-8* (right panel) in *LSD1*-depleted U2OS cells treated with 2 μM etoposide for 7 days was examined by qPCR. (**f**, **g**) U2OS cells treated with 100 nM ORY-1001, a selective irreversible LSD1 inhibitor, and 2 μM etoposide for 7 days were subjected to SA-β-gal (**f**) and EdU (**g**) assays. Representative microscopic images are shown as Fig. S2a,b. (**h**) Gene expression of *p21* in U2OS cells treated with 100 nM ORY-1001 and 2 μM etoposide for 5 days was examined by qPCR (left panel) and immunoblot analysis (right panel). (**i**) Gene expression of *IL-6* (left panel) and *IL-8* (right panel) in U2OS cells treated with 100 nM ORY-1001 and 2 μM etoposide for 6 days was examined by qPCR. (**a**, **d**, **e**, **h**, **i**) qPCR and immunoblot data are representative of three independent experiments and values are shown as mean ± s.e.m. Protein levels relative to γ-tubulin levels were quantified using NIH ImageJ software. Original blots are presented in Supplementary Information. (**b**, **c**, **f**) Data are mean ± s.d. (n = 3 independent cultures). (**g**) Data are mean ± s.d. (n = 4 independent cultures). Statistical significance is shown using Student's *t*-test analysis; $^{*}p < 0.05$; $^{**}p < 0.01$; $^{***}p < 0.005$.

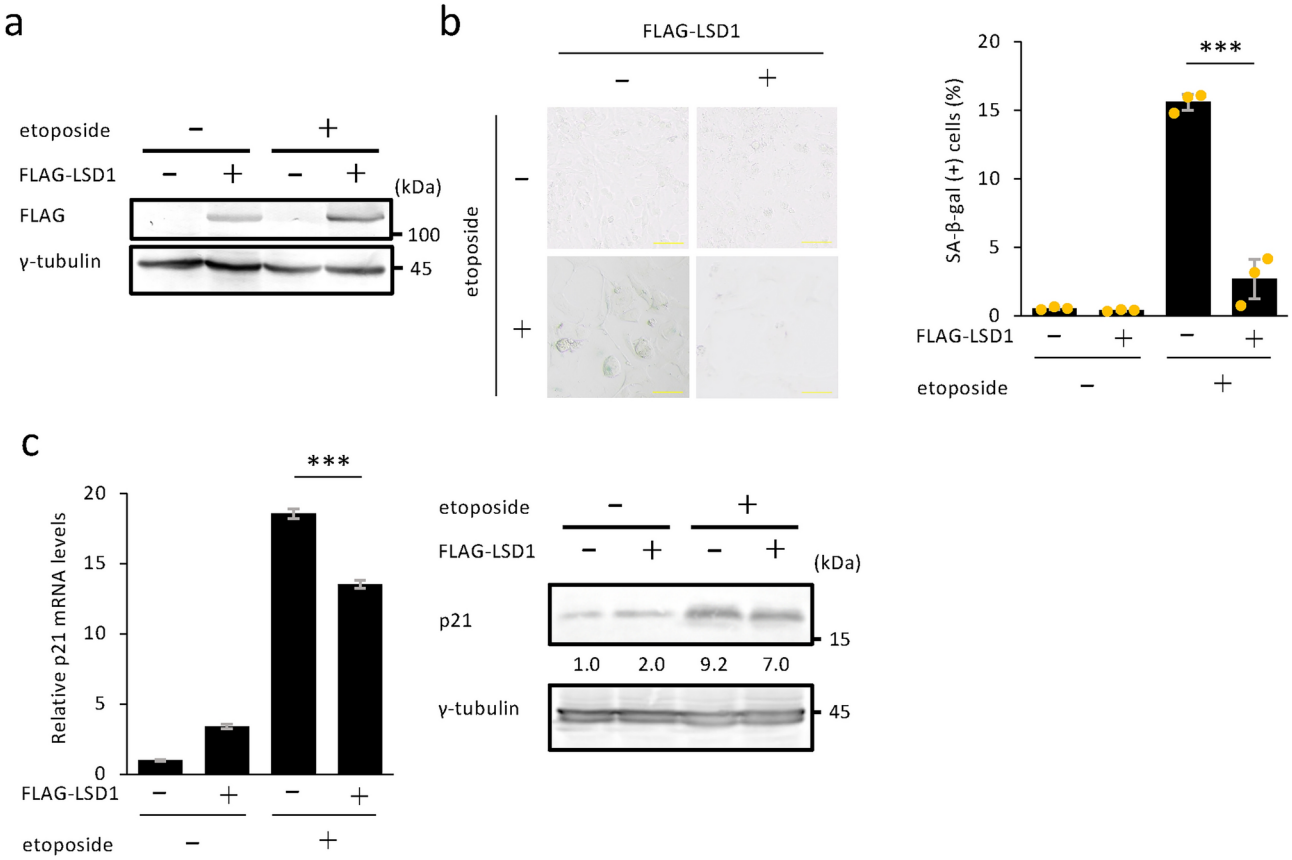

Fig. 2. Overexpression of LSD1 suppresses cellular senescence. (**a**) U2OS cells transfected with p3XFLAG-LSD1 were subjected to immunoblot analysis. Original blots are presented in Supplementary Information. (**b**) LSD1-overexpressing U2OS cells treated with 2 μM etoposide for 7 days were subjected to SA-β-gal assays. Representative microscopic images (left panel) and the percentage of SA-β-gal positive cells (right panel) are shown. Data are mean ± s.d. (n = 3 independent cultures). Bars, 50 μm. (**c**) Gene expression of p21 in LSD1-overexpressing U2OS cells treated with 2 μM etoposide for 5 days were subjected to qPCR (left panel) and immunoblot analysis (right panel). Protein levels relative to γ-tubulin levels were quantified using NIH ImageJ software. Original blots are presented in Supplementary Information. qPCR and immunoblot data are representative of two independent experiments and values are shown as mean ± s.e.m. Statistical significance is shown using Student's *t*-test analysis; ***$p < 0.005$.

levels of H3K4me2 and H3K9me2 were increased (Fig. 3c), suggesting that LSD1 catalytic activity is essential for histone demethylation. Furthermore, we confirmed that, similar to *LSD1* knockdown, LSD1 inhibition also enhanced the expression of *Sirtuin-4* (Fig. 3d). To further confirm the epigenetic modification of histone H3 at the transcriptional regulatory regions of the *Sirtuin-4* gene, we performed chromatin immunoprecipitation (ChIP) experiments (Fig. 3e,f). We constructed primers that could read two regions within 1 kbp from the transcription initiation point of Sirtuin-4. The ChIP-qPCR results showed that inhibition of LSD1 significantly increased H3K4me2 at the promoter site of Sirtuin-4 in etoposide-treated cells but not in untreated cells (Fig. 3e,f). Furthermore, it was found that inhibition of LSD1 activity tended to decrease the binding level of LSD1 to the promoter site of Sirtuin-4. These results also suggest that LSD1 impairs senescence through the epigenetic suppression of *Sirtuin-4*. To further confirm this, we next introduced an expression vector carrying LSD1 into U2OS cells and assessed the methylation levels of histone H3 by immunoblot analysis. In LSD1-overexpressing U2OS cells, demethylation of H3K4me2 and H3K9me2 was promoted after etoposide treatment (Fig. 3g), and concomitantly, *Sirtuin-4* expression was reduced (Fig. 3h). These results suggest that LSD1 is activated in response to senescent stress and suppresses *Sirtuin-4* expression.

Because it has been reported that LSD1 suppresses the DNA binding and transcriptional activity of p53 by removing the dimethyl group at lysine 370 of p53 (p53K370me2)[13], we also analyzed p53 methylation to further clarify the role of LSD1 in suppressing cellular senescence. *LSD1* knockdown and inhibition, which increased the expression of *p21* (Fig. 1d,h), a downstream gene of p53, increased p53K370me2 (Fig. 4a,b). In contrast, LSD1 overexpression, which decreased the expression of p21 (Fig. 2c), decreased p53K370me2 (Fig. 4c). These results suggest that LSD1 activated in response to senescent stress suppresses senescence not only through epigenetic regulation but also possibly through inactivation of p53.

LSD1 is activated by increased uptake of riboflavin

LSD1 is a FAD-dependent demethylase, meaning that FAD is an essential cofactor for LSD1 activity. As previously reported[8], treatment with 50 μM riboflavin inhibits senescence in U2OS cells, as determined by SA-β-gal staining and reduced proliferation capacity. We therefore investigated whether increased riboflavin was sufficient to repress pro-senescence genes through demethylation (Fig. 5a). Addition of riboflavin to etoposide-treated cells only slightly increased intracellular FAD levels (Fig. 5b), so we investigated the intracellular localization of LSD1 and FAD. We found that LSD1 was mainly localized in the nucleus, regardless of the addition of riboflavin (Fig. 5c,d). Interestingly, under the same conditions, the nuclear FAD level was significantly increased (Fig. 5e). These results are consistent with the results of the promotion of demethylation of H3K4me1, H3K4me2, H3K9me1, and H3K9me2 by addition of riboflavin in etoposide-treated cells (Fig. 5f). Furthermore, in etoposide-treated cells, the addition of exogenous riboflavin suppressed the expression of the upregulated senescence-inducing genes *Sirtuin-4* and *p21* (Fig. 5g–i). Because p53 directly controls *p21* expression, the decrease in *p21* expression level is likely due to the inhibition of p53 activity through demethylation caused by LSD1 activation. These results suggest that LSD1 is activated by increased riboflavin uptake in senescent cells.

Activation of LSD1 in senescent cells is regulated by SLC52A1

As previously reported[5,8], the riboflavin transporter SLC52A1 is highly expressed in response to senescent stress and suppresses cellular senescence by increasing intracellular FAD levels. Thus, SLC52A1 may suppress senescence by inhibiting *Sirtuin-4* and *p21* expression via LSD1-mediated demethylation. To investigate this possibility, we transfected U2OS cells with an expression vector carrying SLC52A1. We found that overexpression of SLC52A1 in etoposide-treated cells only slightly increased the total cellular FAD level (Fig. 6a), but increased the nuclear FAD level by more than twofold (Fig. 6b). This result was consistent with the enhanced demethylation of H3K4, H3K9, and p53K370 in etoposide-treated cells, which was reversed by treatment with the LSD1 inhibitor ORY-1001 (Fig. 6c). Furthermore, in etoposide-treated cells, the upregulated expression of *Situin-4* and *p21* was suppressed by overexpression of SLC52A1 (Fig. 6d,e, left panels, and Fig. 6f), which was alleviated by treatment with the LSD1 inhibitor ORY-1001 (Fig. 6d,e, right panels, and Fig. 6f). We next examined whether inhibition of cellular senescence by SLC52A1 was dependent on LSD1 activity. As shown in Figs. 6g,h and S2c,d, etoposide-induced senescence was impaired by SLC52A1 overexpression, which was abolished by LSD1 inhibition. These results suggest that SLC52A1 inhibits senescence via LSD1 activity.

Finally, we examined the effects of *SLC52A1* knockdown on histone and p53 methylation levels and on the expression of *Sirtuin-4* and *p21*. The efficacy of *SLC52A1* knockdown was confirmed by qPCR (Fig. 6i). Knockdown of *SLC52A1* increased methylated H3K4, H3K9 and p53K370 in etoposide-treated cells (Fig. 6j). Moreover, etoposide-induced upregulation of *Sirtuin-4* and *p21* was also promoted by *SLC52A1* knockdown (Fig. 6k–m). Taken together, these results suggest that LSD1 is activated by riboflavin internalized by SLC52A1, which is upregulated in senescent cells, and suppresses cellular senescence by regulating the expression of downstream senescence-inducing genes, such as *Sirtuin-4* and *p21* (Fig. 7).

Discussion

As previously reported[5], sublethal doses of the DNA-damaging anticancer drug etoposide induce cellular senescence in human osteosarcoma cell line U2OS cells and human foreskin fibroblasts Hs68 cells. Meanwhile, LSD1 has been reported to suppress replicative senescence in trophoblast stem cells[11] and glioblastoma cells[16], as well as Ras-induced senescence in mouse embryo fibroblasts[17]. To our knowledge, LSD1 can inhibit senescence induced by some stresses, but it is unclear whether LSD1 inhibits senescence induced by DNA damage. Our results showed that LSD1 suppresses senescence induced by etoposide treatment in U2OS cells as measured by widely used senescence markers. Furthermore, we found that LSD1 inhibition promotes senescence induced by etoposide treatment in Hs68 cells. These results, together with previous reports by other investigators, suggest that LSD1 suppresses senescence in various cell lines induced by various stresses, including DNA damage caused by etoposide treatment.

The riboflavin transporter SLC52A1 is upregulated in response to senescence-inducing stimuli and contributes to the suppression of senescence[5]. Furthermore, the intracellular levels of FAD converted from riboflavin are increased by upregulation of SLC52A1[8], raising the possibility that FAD-dependent enzymes are key components for the mechanism by which SLC52A1 inhibits senescence. We have previously discovered that activation of mitochondrial ETC complex II, which contains FAD-dependent succinate dehydrogenase, by inducing SLC52A1 expression contributes to the suppression of senescence[8]. However, ETC complex II alone cannot completely suppress cellular senescence, so the complete mechanism by which SLC52A1 suppresses senescence remains to be elucidated. In this study, we found that LSD1 is activated in response to senescent stress. Furthermore, increased intracellular FAD and upregulated SLC52A1 promoted LSD1 activation, and LSD1 inhibition abrogated SLC52A1-dependent suppression of senescence. This suggests that LSD1 activated by increased intracellular FAD due to upregulated SLC52A1 suppresses cellular senescence.

Our previous report demonstrated the negative feedback regulation of p53 via SLC52A1[8], and showed that elevated FAD levels in senescent cells lead to activation of mitochondrial membrane potential, suppressing the AMPK-p53-p21 pathway and inhibiting p53-dependent senescence. In this study, we proposed that LSD1 inhibits senescence not only by suppressing *Sirtuin-4* but also by demethylating p53K370me2 and suppressing *p21*, a key mediator of p53-dependent cell cycle arrest and a marker of senescence[18,19]. Because LSD1 suppresses p53-mediated transcriptional activation by demethylating K370 of p53[13], SLC52A1-mediated inhibition of senescence may be mediated by both the AMPK-p53 pathway and the LSD1-p53 pathway.

In human cells, in addition to *Sirtuin-4* and *p53*, there are many downstream genes regulated by LSD1 that are involved in cell cycle and cellular senescence. For example, LSD1 promotes the expression of E2F1 target genes such as *MYC* and *AKT3* and induces transition to S-phase[12], so it may be involved in SLC52A1-dependent

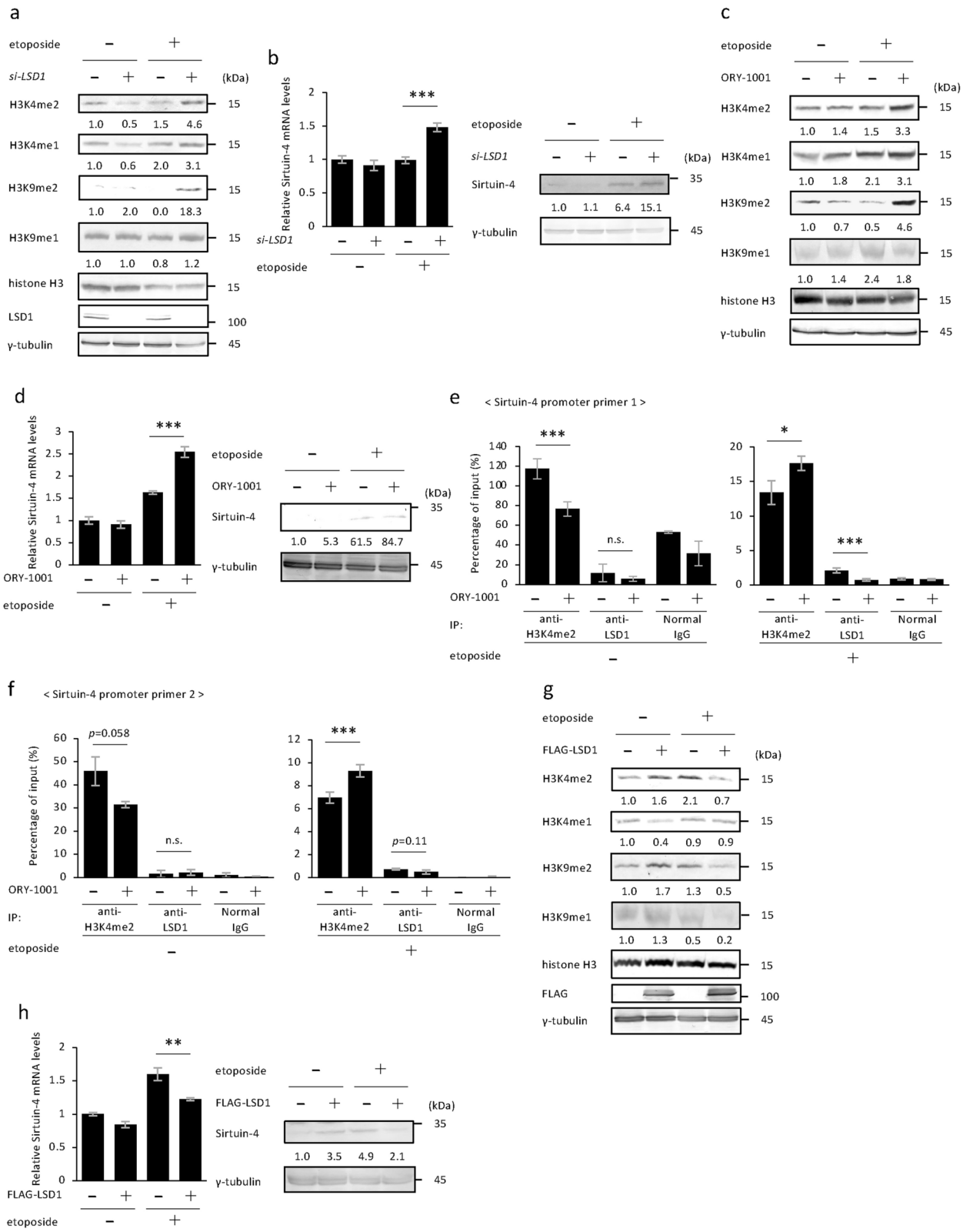

senescence suppression mechanism. It is hoped that the new anti-senescence mechanism we discovered will lead to further treatments for age-related diseases.

Proteins that use FMN or FAD, synthesized from riboflavin, as cofactors are called flavoproteins, and the human genome encodes more than 90 types of flavoproteins[20]. Increased riboflavin uptake in senescent cells may activate many flavoproteins. We previously reported that PRODH and DAO are flavoproteins activated in senescent cells, which generate ROS as by-products during amino acid metabolism and promote cellular senescence[21,22]. On the other hand, ETC complex II, which is activated by increased FAD in senescent cells[8], and LSD1, as identified in this study, suppress cellular senescence. In other words, in senescent cells, promotion

◂**Fig. 3**. LSD1 is activated in response to senescent stress. (**a**) U2OS cells transfected with siRNA for *LSD1* and treated with 2 μM etoposide for 5 days were subjected to immunoblot analysis. (**b**) U2OS cells transfected with siRNA for *LSD1* and treated with 2 μM etoposide for 7 days were subjected to qPCR (left panel) and immunoblot analysis (right panel). (**c**) U2OS cells treated with 100 nM ORY-1001 and 2 μM etoposide for 5 days were subjected to immunoblot analysis. (**d**) U2OS cells treated with 100 nM ORY-1001 and 2 μM etoposide for 7 days were subjected to qPCR (left panel) and immunoblot analysis (right panel). (**e**, **f**) U2OS cells treated with 100 nM ORY-1001 and 2 μM etoposide for 6 days were subjected to ChIP-qPCR analysis to measure H3K4me2 and LSD1 bound to the *Sirtuin-4* promoter sites. (**g**) U2OS cells transfected with p3XFLAG-LSD1 and treated with 2 μM etoposide for 5 days were subjected to immunoblot analysis. (**h**) U2OS cells transfected with p3XFLAG-LSD1 and treated with 2 μM etoposide for 7 days were subjected to qPCR (left panel) and immunoblot analysis (right panel). Protein levels relative to histone H3 levels (**a**, **c**, **g**) or γ-tubulin levels (**b**, **d**, **h**, right panel) were quantified using NIH ImageJ software. Original blots are presented in Supplementary Information. Data are representative of three (**a**, **c**, **g**) or two (**b**, **d**, **h**, right panel) independent experiments and values are shown as mean ± s.e.m. Statistical significance is shown using Student's *t*-test analysis; $^{*}p < 0.05$; $^{**}p < 0.01$; $^{***}p < 0.005$; n.s., not significant ($p > 0.05$).

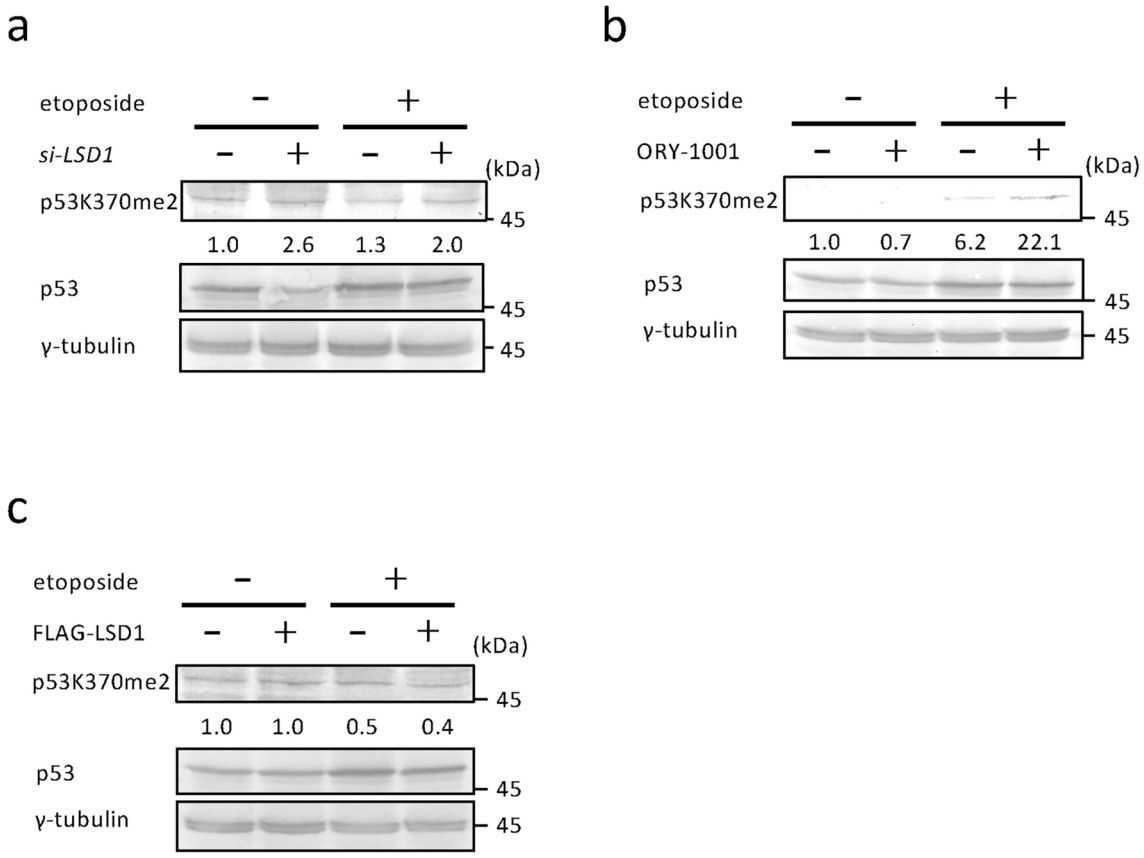

Fig. 4. LSD1 demethylates p53 in response to senescent stress. (**a**) U2OS cells transfected with siRNA for *LSD1* and treated with 2 μM etoposide for 5 days were subjected to immunoblot analysis. (**b**) U2OS cells treated with 100 nM ORY-1001 and 2 μM etoposide for 5 days were subjected to immunoblot analysis. (**c**) U2OS cells transfected with p3XFLAG-LSD1 and treated with 2 μM etoposide for 5 days were subjected to immunoblot analysis. Protein levels relative to p53 levels were quantified using NIH ImageJ software. Original blots are presented in Supplementary Information. Data are representative of two independent experiments and values are shown as mean ± s.e.m.

and inhibition are simultaneously regulated by multiple flavoproteins, and whether promotion or inhibition occurs may differ depending on the cell type and the environment in which the cell is placed. To elucidate the mechanism of cellular senescence control, detailed analysis of proteins whose activities are regulated by riboflavin may be necessary.

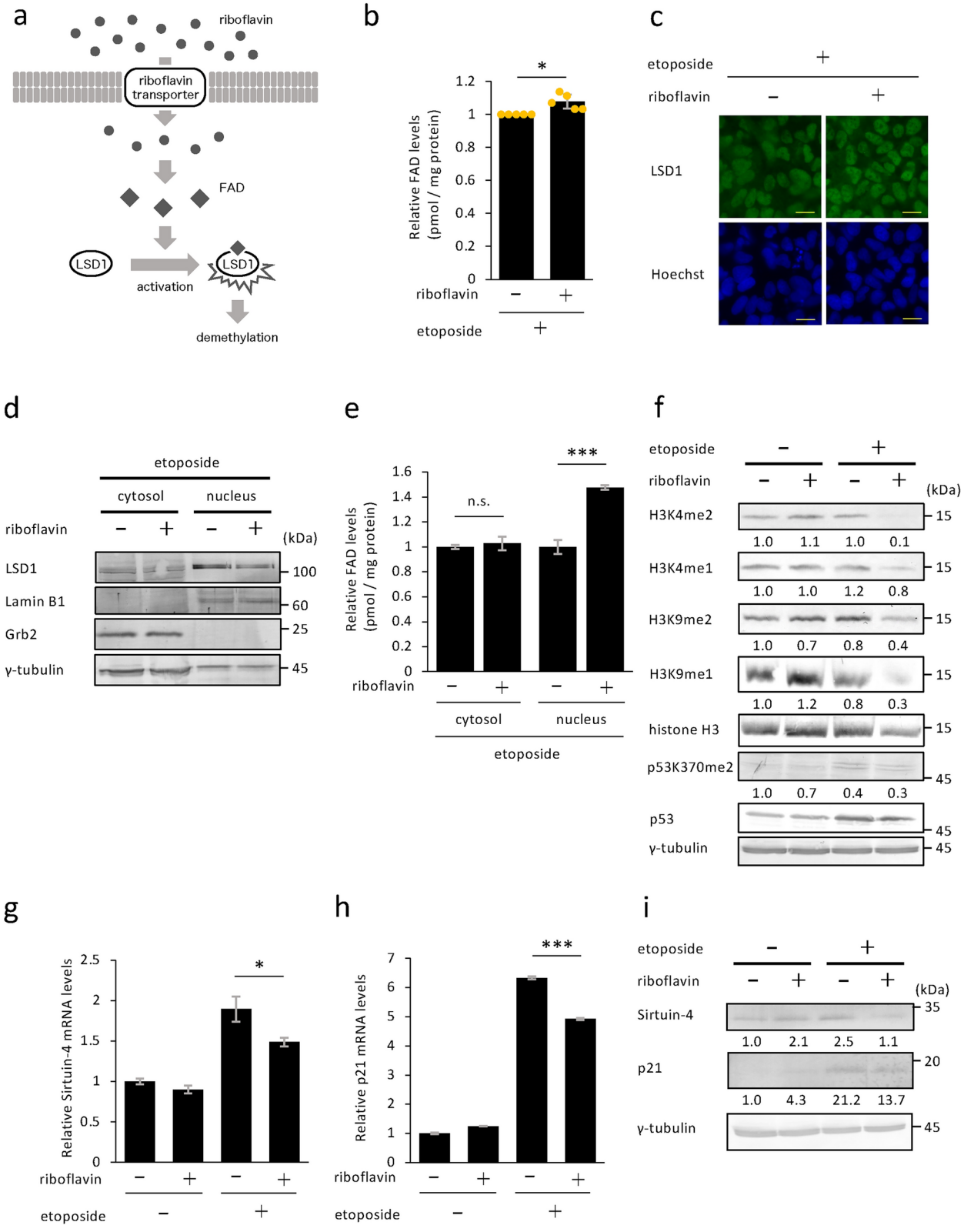

Methods

Cell culture, treatment, and transfection

U2OS cells (a human osteosarcoma line; American Type Culture Collection, Rockville, MD) and Hs68 cells (normal human diploid fibroblasts; IFO50350; JCRB Cell Bank, Osaka, Japan) were cultured in DMEM (Wako, Osaka, Japan) supplemented with 10% fetal bovine serum. The cells were treated with etoposide (Sigma Aldrich, St. Louis, MO) to induce DNA double-strand breaks. For senescence induction, both U2OS and Hs68 cells were treated with 2 μM etoposide (Sigma Aldrich) for 48 h and then cultured in DMEM without etoposide for an additional 5 days to develop senescence phenotypes[5,8,23]. Transfection with expression vectors was performed

◀**Fig. 5**. LSD1 is activated by increased riboflavin uptake. (**a**) Schematic diagram of LSD1 activation by the riboflavin transporter. Riboflavin uptake may lead to increase FAD and activate LSD1. (**b**) U2OS cells treated with 50 μM riboflavin and 2 μM etoposide for 2 days were subjected to measurement of intracellular FAD levels. Data are mean ± s.d. (n = 5 independent cultures). (**c**-**e**) U2OS cells treated with 50 μM riboflavin and 2 μM etoposide for 2 days were subjected to immunofluorescence (**c**), cell fractionation (**d**), and measurement of FAD levels in each fraction (**e**). Bars, 20 μm. (**f**) U2OS cells treated with 50 μM riboflavin and 2 μM etoposide for 3 days were subjected to immunoblot analysis. Protein levels relative to histone H3 or p53 levels were quantified using NIH ImageJ software. (**g**–**i**) U2OS cells treated with 50 μM riboflavin and 2 μM etoposide for 4 days were subjected to qPCR (**g** and **h**) and immunoblot analysis (**i**). Protein levels relative to γ-tubulin levels were quantified using NIH ImageJ software. qPCR and immunoblot data are representative of three (**f**) or two (**g**–**i**) independent experiments and values are shown as mean ± s.e.m. Original blots are presented in Supplementary Information. Statistical significance is shown using Student's *t*-test analysis; $^{*}p < 0.05$; $^{***}p < 0.005$; n.s., not significant ($p > 0.05$).

using Effectene Transfection Reagent (Qiagen, Venlo, the Netherlands) according to the manufacturer's instructions. The transfected cells were selected by 800 μg/mL of the neomycin analogue G418 (Wako) for 5 days. Riboflavin (Nacalai Tesque, Kyoto, Japan) was added to the medium to 50 μM. When ORY-1001 (Cayman Chemical) was used, the reagent was added at 100 nM. Stock solutions of etoposide were prepared in dimethyl sulfoxide. Riboflavin was dissolved in 100 mM NaOH, whereas ORY-1001 was dissolved in DW.

Plasmid constructions

For the construction of p3XFLAG-CMV-10-LSD1, an expression vector for N-terminal FLAG-tagged human full-length LSD1 (NCBI Reference Sequence: NM_015013.4), the cDNA fragment of LSD1 was amplified with a pair of primers (a forward primer: 5′-GACAAGCTTGCGGCCTTATCTGGGAAGAAGGCGG-3′ and a reverse primer: 5′-GATGAATTCGCGGCCTCACATGCTTGGGGACTG-3′) using a cDNA sample prepared from U2OS as a template. The resultant fragment was digested with NotI and cloned into the p3XFLAG-CMV-10 vector (Sigma-Aldrich). To generate pcDNA3-HA-SLC52A1, an expression vector for N-terminal HA-tagged human full-length SLC52A1 (NCBI Reference Sequence: NM_001104577.2), the cDNA fragment of SLC52A1 was amplified with a pair of primers (a forward primer: 5′-CGTGCTCGGAATTCATGGCAGCACCCACG CT-3′ and a reverse primer: 5′-CGTGATAGGCGGCCGCTCAGGGGCCACAGGGGT-3′) using a plasmid containing PAR2 (SLC52A1) cDNA (kindly provided by Y. Takeuchi, University College London, UK) as a template. The resulting PCR fragment was digested with EcoRI and NotI and cloned into the pcDNA3 vector (Invitrogen, Carlsbad, CA).

Immunoblot analysis

The cells were lysed in lysis buffer (1% Triton X-100, 20 mM Tris–HCl [pH 7.5], 1 mM EDTA, 1 mM EGTA, 150 mM NaCl, 10 mM 2-mercaptoethanol, 5 μg/ml leupeptin, 20 μM APMSF, 1 mM Na3VO4), and the lysates were separated by SDS–PAGE and blotted onto Immobilon polyvinylidene difluoride membrane (Merck Millipore, Darmstadt, Germany). Each protein was detected using primary antibodies as indicated, alkaline phosphatase (AP)-conjugated secondary antibodies, and the chromogenic NBT/BCIP (Nacalai Tesque) substrates.

Immunofluorescence analysis

For immunofluorescence analysis, the cells were fixed with 3.7% formaldehyde and permeabilized in 0.5% Triton X-100 and then incubated with primary antibodies for 1 h at room temperature, followed by incubation with the Alexa Fluor 488—conjugated secondary antibody (Life Technologies) for 1 h at room temperature. After staining cell nuclei with Hoechst 33258, the cells were observed under fluorescence microscope (model BZ-9000; Keyence, Osaka, Japan).

Antibodies

Anti-FLAG M2 monoclonal antibody (F3165) and anti-γ-tubulin antibody (T6557) were obtained from Sigma Aldrich; anti-Histone H3 (D1H2) antibody (#4499T), anti-Di-Methyl-Histone H3 (Lys4) (C64G9) antibody (#9725 T), anti-Mono-Methyl-Histone H3 (Lys9) (D1P5R) antibody (#14186), anti-Di-Methyl-Histone H3 (Lys9) (D85B4) antibody (#4658T), anti-Sirtuin-4 antibody (#69786) were from Cell Signaling Technology (Beverly, MA); anti-LSD1 antibody (ab69535), anti-H3K4me1 antibody (ab8895) were from Abcam; anti-Di-Methyl-p53 (K370) antibody (STJ90115) was from St John's Laboratory Ltd. (London, UK); anti-p21 antibody (sc-56335), anti-p53 antibody (sc-126), anti-Lamin B1 antibody (sc-6217) were from Santa Cruz Biotechnology (Santa Cruz, CA); anti-Grb2 antibody (G16720) was from BD Biosciences (Franklin Lakes, NJ); anti-phospho-Histone H2A.X (Ser139) antibody (05-636) was from Merck Millipore (Burlington, MA); AP-conjugated anti-mouse antibody (S372B) and AP-conjugated anti-rabbit antibody (S373B) were from Promega (Madison, WI).

Senescence assay

To measure SA-β-gal activity, the Senescence β-Galactosidase staining kit (Cell Signaling Technology) was used according to the manufacturer's instructions. Briefly, the cells were fixed with 2% formaldehyde/0.2% glutaraldehyde for 15 min and then stained with SA-β-Gal staining solution (1 mg/ml 5-bromo-4-chloro-3-indolyl-β-D-galactoside, 40 mM citric acid/sodium phosphate [pH 6.0], 5 mM potassium ferrocyanide, 5 mM potassium ferricyanide, 150 mM NaCl, 2 mM MgCl2) for 24 h at 37℃. The stained cells were examined under

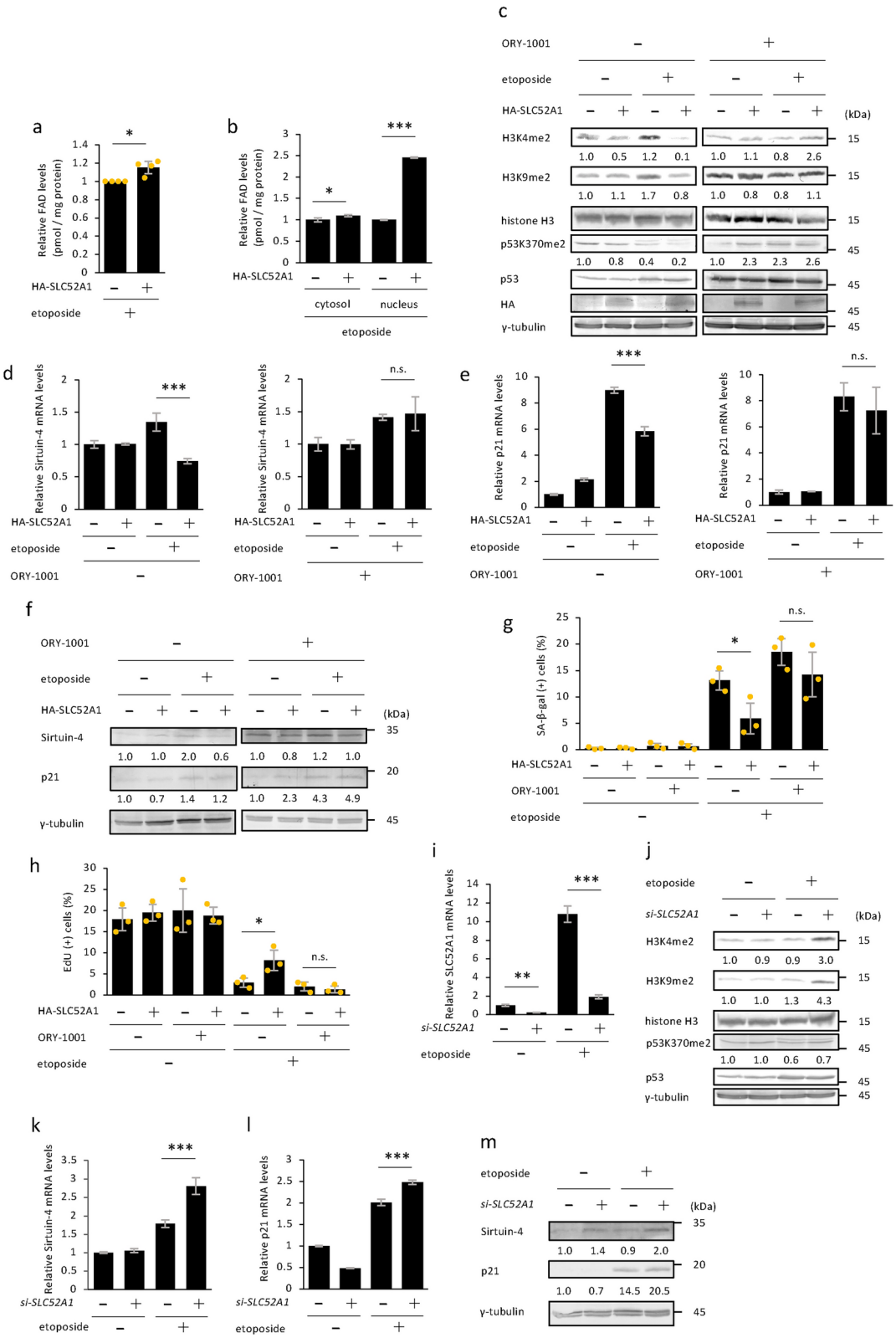

a fluorescence microscope (model BZ-8000; Keyence, Osaka, Japan), and blue-stained cells were identified as senescent. For the EdU incorporation proliferation assay, the cells were labeled with 10 μM EdU for 3 h (U2OS cells) or 24 h (Hs68 cells) and then EdU incorporation was visualized by using Click-iT EdU Imaging Kit (Life Technologies) according to the manufacturer's instructions. The stained cells were observed under a fluorescence microscope (model BZ-9000; Keyence, Osaka, Japan). At least 100 cells were counted in each of three randomly selected microscopic fields, and the percentages of SA-β-gal- and EdU-positive cells were determined.

◀**Fig. 6**. LSD1 is activated by SLC52A1 overexpression. (**a**) U2OS cells transfected with pcDNA3-HA-SLC52A1 and treated with 2 μM etoposide for 24 h were subjected to measurement of intracellular FAD levels. Data are mean ± s.d. (n = 4 independent cultures). (**b**) U2OS cells transfected with pcDNA3-HA-SLC52A1 and treated with 2 μM etoposide for 24 h were subjected to cell fractionation and measurement of FAD levels in each fraction. (**c**) SLC52A1-overexpressing U2OS cells treated with 2 μM etoposide and 100 nM ORY-1001 for 24 h were subjected to immunoblot analysis. Protein levels relative to histone H3 or p53 levels were quantified using NIH ImageJ software. (**d**–**f**) SLC52A1-overexpressing U2OS cells treated with 2 μM etoposide without (**d** and **e**, left panels) or with (**d** and **e**, right panels) 100 nM ORY-1001 for 24 h was examined by qPCR and immunoblot analysis (**f**). (**g**, **h**) SLC52A1-overexpressing U2OS cells treated with 2 μM etoposide and 100 nM ORY-1001 for 7 days were subjected to SA-β-gal (**g**) and EdU (**h**) assays. The percentage of SA-β-gal positive cells (**g**) and EdU positive cells (**h**) are shown. Data are mean ± s.d. (n = 3 independent cultures). Representative microscopic images are shown as Fig. S2c,d. (**i**) U2OS cells transfected with siRNA for SLC52A1 and treated with 2 μM etoposide for 2 days were subjected to qPCR. (**j**) SLC52A1-depleted U2OS cells treated with 2 μM etoposide for 2 days were subjected to immunoblot analysis. Protein levels relative to histone H3 or p53 levels were quantified using NIH ImageJ software. Original blots are presented in Supplementary Information. (**k**–**m**) SLC52A1-depleted U2OS cells treated with 2 μM etoposide for 2 days were subjected to qPCR (**k** and **l**) and immunoblot analysis (**m**). (**c**–**f**) qPCR and immunoblot data are representative of two independent experiments and values are shown as mean ± s.e.m. (**c**, **f**, **j**, **m**) Protein levels relative to histone H3 levels (**c**, **j**), p53 levels (**c**, **j**) or γ-tubulin levels (**f**, **m**) were quantified using NIH ImageJ software. Original blots are presented in Supplementary Information. Statistical significance is shown using Student's *t*-test analysis; $^{*}p < 0.05$; $^{***}p < 0.005$; n.s., not significant ($p > 0.05$).

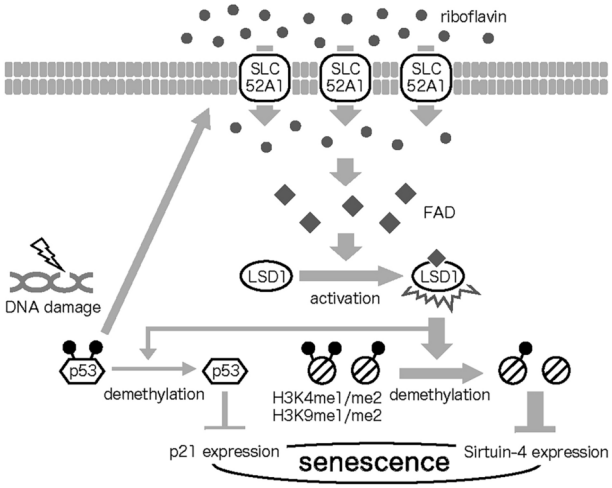

Fig. 7. LSD1 suppresses cellular senescence by inhibiting the expression of Sirtuin-4 and p21. Schematic diagram of LSD1 activation by SLC52A1. SLC52A1 contributes to increased riboflavin uptake upon DNA damage, activates LSD1 by increasing FAD levels, and ultimately inhibits cellular senescence by downregulating the expression of senescence-inducing genes such as *Sirtuin-4* and *p21*.

RNA interference

ON-TARGETplus Smart Pool siRNA for *SLC52A1* (L-010712-00) and *LSD1* (L-009223-00-0005) and their control siRNA (D-001810–10) were from Dharmacon Horizon Discovery (Lafayette, CO). U2OS and Hs68 cells were seeded and transfected with 30 nM siRNA using Lipofectamin RNAiMAX Transfection Reagent (ThermoFisher Scientific) according to the manufacturer's instructions.

RNA isolation and quantitative PCR (qPCR)

Total RNA was isolated from siRNA-transfected U2OS and Hs68 cells using the RNeasy Mini Kit (Qiagen) according to the manufacturer's instructions. cDNA was synthesized using the ReverTra Ace qPCR RT Master Mix with gDNA Remover (TOYOBO, Osaka, Japan) and subjected to qPCR (LightCycler480 Real-Time PCR System; Roche Life Science, Penzberg, Germany) using specific primers for GAPDH (a forward primer: 5′-CAATGACCCCTTCATTGACCT-3′ and a reverse primer: 5′-ATGACAAGCTTCCCGTTCTC-3′), LSD1 (a forward primer: 5′-TTCTCAAGAAGCAGCCTG-3′ and a reverse primer: 5′-TGCAGATGTTTTCCACTCAG-3′), p21 (a forward primer: 5′-CGACTGTGATGCGCTAATG-3′ and a reverse primer: 5′-TCTCGGTGACAAAGTCGAAG-3′), IL-6 (a forward primer: 5′-GGGCACCTCAGATTGTTGTT-3′ and a reverse primer: 5′-GTGCCCAGTGGACAGGTTT-3′), IL-8 (a forward primer: 5′-CTGTGTGAAGGTGCAGTTTTG-3′ and a reverse primer: 5′-TCTGTGTTGGCGCAGTGT-3′), MMP1 (a forward primer: 5′-CTGGCCACAACTGCCAAATG-3′ and a reverse primer: 5′-CTGTCCCTGAACAGCCCAGTACTTA-3′), MMP3 (a forward primer: 5′-TGGACAAAGGATACAACAGGGAC-3′ and a reverse primer: 5′-AGCTTCAGTGTTGGCTGAGT-3′), Sirtuin-4

(a forward primer: 5′-GGGGTGTGAAGTGTCCGTAG-3′ and a reverse primer: 5′-ACCCAATGGAGGCTTTCGAG-3′), and SLC52A1 (a forward primer: 5′-TTGCTGTTGCCATCACTACC-3′ and a reverse primer: 5′-CAAAGCCTCTTCTTCCTCCTTC-3′). Relative expression levels were calculated by the $2^{(\Delta\Delta Ct)}$ method (ΔCt sample–ΔCt calibrator).

Chromatin immunoprecipitation assay

To perform chromatin immunoprecipitation, CUT&RUN Assay Kit (Cell Signaling Technology) was used according to the manufacturer's instructions. DNA fragments were precipitated using anti-H3K4me2 and anti-LSD1 antibodies. The amount of DNA fragments bound to the target protein was analyzed by qPCR using specific primers for Sirtuin-4 promoter primer 1 (a forward primer: 5′-GGAAGAGGCTGGTGTAGTGG-3′ and a reverse primer: 5′-TGCCCCTAGTGTGGTACTTG-3′), and Sirtuin-4 promoter primer 2 (a forward primer: 5′-TACCACACTAGGGGCAAGAGA-3′ and a reverse primer: 5′-GGCAGAGCTGGGGCTTATC-3′).

FAD measurement

FAD measurement was performed using the FAD Assay Kit (ab204710; Abcam, Cambridge, UK) according to the manufacturer's instructions. Briefly, the cells were lysed and deproteinized with $HClO_4$, and the resulting samples were mixed with the reaction mixture. FAD concentrations were measured by a colorimetric assay at 570 nm based on the FAD-dependent reaction of the OxiRed probe using a spectrophotometer (iMark microplate reader; Bio-Rad, Hercules, CA).

Cell fractionation

To obtain cell nuclear fractions, cells were lysed in hypotonic buffer (20 mM HEPES [pH7.5], 5 mM NaF, 100 μM EDTA, 10 μM Na_2MoO_4), then NP40 was added, pipetted thoroughly, and centrifuged at 2000 rpm for 5 min. The supernatant was collected to obtain the cytoplasmic fraction. Furthermore, the precipitate was dissolved in a SDS-containing Hypotonic buffer (1% SDS, 0.3% NP40), centrifuged at 5000 rpm for 15 min. The supernatant was collected to obtain the cell nuclear fraction. When measuring the amount of FAD in the nuclear fraction, FAD Assay Buffer (included in the FAD Assay Kit) was used instead of the SDS-containing Hypotonic buffer.

Statistical analysis

The two-tailed Student's *t*-test was used to calculate *p*-values for all datasets.

Data availability

The datasets used and/or analysed during the current study available from the corresponding author on reasonable request. All data generated or analysed during this study are included in this published article and its supplementary information files.

Received: 30 September 2024; Accepted: 17 February 2025
Published online: 23 February 2025

References

1. Campisi, J. Aging, cellular senescence, and cancer. *Annu. Rev. Physiol.* **75**, 685–705 (2013).
2. Salama, R., Sadaie, M., Hoare, M. & Narita, M. Cellular senescence and its effector programs. *Genes Dev.* **28**, 99–114 (2014).
3. Yang, J. H. et al. Loss of epigenetic information as a cause of mammalian aging. *Cell* **186**, 305-326.e27 (2023).
4. van Deursen, J. M. Senolytic therapies for healthy longevity. *Science* **364**, 636–637 (2019).
5. Nagano, T. et al. Identification of cellular senescence-specific genes by comparative transcriptomics. *Sci. Rep.* **6**, 31758 (2016).
6. Powers, H. J. Riboflavin (vitamin B-2) and health. *Am. J. Clin. Nutr.* **77**, 1352–1360 (2003).
7. Udhayabanu, T. et al. Riboflavin responsive mitochondrial dysfunction in neurodegenerative diseases. *J. Clin. Med.* **6**, 52 (2017).
8. Nagano, T. et al. Riboflavin transporter SLC52A1, a target of p53, suppresses cellular senescence by activating mitochondrial complex II. *Mol. Biol. Cell* **32**, br10 (2021).
9. Shi, Y. et al. Histone demethylation mediated by the nuclear amine oxidase homolog LSD1. *Cell* **119**, 941–953 (2004).
10. Thinnes, C. C. et al. Targeting histone lysine demethylases - progress, challenges, and the future. *Biochim. Biophys. Acta* **1839**, 1416–1432 (2014).
11. Castex, J. et al. Inactivation of Lsd1 triggers senescence in trophoblast stem cells by induction of Sirt4. *Cell Death Dis.* **8**, e2631 (2017).
12. He, Y. et al. LSD1 promotes S-phase entry and tumorigenesis via chromatin co-occupation with E2F1 and selective H3K9 demethylation. *Oncogene* **37**, 534–543 (2018).
13. Huang, J. et al. p53 is regulated by the lysine demethylase LSD1. *Nature* **449**, 105–108 (2007).
14. Dimri, G. P. et al. A biomarker that identifies senescent human cells in culture and in aging skin in vivo. *Proc. Natl. Acad. Sci. USA* **92**, 9363–9367 (1995).
15. Maes, T. et al. ORY-1001, a potent and selective covalent KDM1A inhibitor, for the treatment of acute Leukemia. *Cancer Cell* **33**, 495–511 (2018).
16. Saccà, C. D. et al. Inhibition of lysine-specific demethylase LSD1 induces senescence in Glioblastoma cells through a HIF-1α-dependent pathway. *Biochim. Biophys. Acta Gene Regul. Mech.* **1862**, 535–546 (2019).
17. Yu, Y. et al. Targeting the senescence-overriding cooperative activity of structurally unrelated H3K9 demethylases in melanoma. *Cancer Cell* **33**, 322-336.e8 (2018).
18. El-Deiry, W. S. et al. WAF1, a potential mediator of p53 tumor suppression. *Cell* **75**, 817–825 (1993).
19. Romanov, V. S., Pospelov, V. A. & Pospelova, T. V. Cyclin-dependent kinase inhibitor p21(Waf1): Contemporary view on its role in senescence and oncogenesis. *Biochemistry (Mosc)* **77**, 575–584 (2012).
20. Tolomeo, M., Nisco, A., Leone, P. & Barile, M. Development of novel experimental models to study flavoproteome alterations in human neuromuscular diseases: The effect of rf therapy. *Int. J. Mol. Sci.* **21**, 5310 (2020).
21. Nagano, T. et al. Proline dehydrogenase promotes senescence through the generation of reactive oxygen species. *J. Cell Sci.* **130**, 1413–1420 (2017).
22. Nagano, T. et al. D-amino acid oxidase promotes cellular senescence via the production of reactive oxygen species. *Life Sci. Alliance* **2**, e201800045 (2019).

23. Nakano, M. et al. Branched-chain amino acids enhance premature senescence through mammalian target of rapamycin complex I-mediated upregulation of p21 protein. *PLoS One* **8**, e80411 (2013).

Acknowledgements
We thank Y. Takeuchi for providing the PAR2 (SLC52A1) plasmid.

Author contributions
S. K. conceived and designated the experiments. T. O. performed the experiments. T. O. and T. N. analyzed the data. T. O., T. N., T. I., J. N., K. M., and S. K. contributed reagents/materials/analysis tools. T. O. and S. K. wrote the manuscript. All authors reviewed the results and approved the final version of the manuscript.

Declarations

Competing interests
The authors declare no competing interests.

Additional information
Supplementary Information The online version contains supplementary material available at https://doi.org/10.1038/s41598-025-91004-0.

Correspondence and requests for materials should be addressed to S.K.

Reprints and permissions information is available at www.nature.com/reprints.

Publisher's note Springer Nature remains neutral with regard to jurisdictional claims in published maps and institutional affiliations.